THE JOURNAL OF PHYSICAL CHEMISTRY C LETTERS

2007, *111,* 16076−16079
Published on Web 10/05/2007

Mechanisms of Spectral Profile Modification in Surface-Enhanced Fluorescence

E. C. Le Ru* and P. G. Etchegoin

The MacDiarmid Institute for Advanced Materials and Nanotechnology, School of Chemical and Physical Sciences, Victoria University of Wellington, P.O. Box 600, Wellington, New Zealand

J. Grand, N. Félidj, J. Aubard, and G. Lévi

Laboratoire ITODYS, Université Paris 7 − Denis Diderot, CNRS UMR 7086, 1 rue Guy de la Brosse, F - 75005 Paris, France

Received: July 29, 2007; In Final Form: September 2, 2007

We study the importance of an often-overlooked aspect of surface-enhanced fluorescence (SEF): the spectral profile modification (SPM) that should accompany any plasmon-resonance-mediated enhancement or quenching of the fluorescence close to metal surfaces. We argue theoretically and demonstrate experimentally that under SEF conditions the plasmon resonances affect not only the fluorescence intensity (enhancement or quenching) but also its spectral profile, sometimes to a point where the original fluorescence spectrum may no longer be recognizable as such. Moreover, we argue that the modified excited-state decay rate may, under certain conditions, become comparable to the internal relaxation rate. This effect leads to a new fluorescence mechanism, which we call fast-dynamics SEF (FDSEF), where the spectral profile is affected by the relaxation dynamics in the excited state (in addition to the plasmon resonance). Finally, we propose that the so-called surface-enhanced Raman scattering (SERS) continuum may, in many instances, be interpreted in terms of a SPM of the SEF (in its simplest form or as FDSEF). Experimental evidence using highly uniform nanolithography-prepared gold nanostructures are provided to support these ideas.

The theory of surface-enhanced fluorescence (SEF), along with more advanced concepts, was developed extensively in the 1970−1980s.[1−4] However, it is only recently (with the renewed interest in plasmonics) that experimental advances have allowed to clearly confirm various aspects of these theories[5−8] and foresee more elaborate applications. SEF consists of a modification (quenching or enhancement) of the fluorescence intensities and lifetimes for molecules adsorbed on (or at least close to, by a few nanometers) a metal surface. This arises from the strong electromagnetic (EM) response of metallic objects, particularly when localized surface plasmon (LSP) resonances are excited.[2−4,9,10] A large quenching or enhancement of the fluorescence can be observed depending on the exact conditions, and this can be understood within classical EM theory;[2−4] further confirmed by quantum studies.[1,11] In most of these models, the emitter is depicted as a simple two- (or three-) level system; that is, only one emission wavelength is considered. This is appropriate in general to understand modifications of absorption or emission rates, but it entirely ignores the spectral profile of the fluorescence emission.

There are other situations where a modification of the fluorescence spectrum is known to occur. Examples include the following: (i) the formation of dye aggregates, such as J-aggregates,[12] (ii) a modification of the chemical (and therefore electronic) properties of the fluorophore upon adsorption (in particular chemisorption) on a metal surface (through a charge-transfer mechanism for example[13]), and (iii) a shift of the fluorophore energy levels as a result of electromagnetic interactions with a metal surface.[14,15] In all of these cases, the fluorescence spectral profile is changed as a result of a modification of the energy levels of the emitter. We ignore any such effects here and argue that a spectral profile modification (SPM) of the fluorescence can still occur in general conditions close to metallic surfaces through the same mechanisms as those that cause SEF, even when the electronic energy levels are not affected by adsorption. This may act in addition to any other mechanisms affecting the energy levels directly. Such small SPM of the metal luminescence[16] or fluorescence[6,17] have already been reported, and we will argue in this letter that much more dramatic modifications can be observed.

Hence, we discuss here the extension of one of the simplest forms of the SEF model to incorporate the spectral profile of the fluorescence. We predict at least two distinct regimes where an SPM can be expected; we call them slow-dynamics SEF (SDSEF) and fast-dynamics (FDSEF), depending on the magnitude of the modified decay rate Γ_{Tot} of the excited state. SDSEF corresponds to the "common" view of SEF. FDSEF, which occurs when Γ_{Tot} is comparable to internal energy relaxation rate, is to our knowledge a new concept. In both regimes, the SPM occurs mostly independent of the accompanying enhancement or quenching of the fluorescence intensity. The spectral profile may, in fact, be modified sufficiently to make it difficult to recognize the original spectrum experimentally. This is probably one of the reasons that this effect has

* Corresponding author. E-mail address: Eric.LeRu@vuw.ac.nz.

10.1021/jp076003g CCC: $37.00

not yet been studied in detail; it has most likely been observed many times but not identified as such. To support our claims, we carry out surface-enhanced Raman scattering (SERS) experiments on well-defined SERS substrates. SERS occurs in conjunction with SEF and, therefore, allows us to monitor it effectively. Our experimental results show that SEF is common under typical SERS conditions, and we argue that SEF, as SDSEF and/or FDSEF, could account for the debated[17,21−23] *SERS continuum* in many common situations.

To understand the two mechanisms of SPM in SEF, we will use a classical EM description of SEF and, for the sake of clarity, make as many simplifications as possible while retaining the features we want to highlight. Accordingly, we will ignore any vectorial, tensorial, or orientational effects, which can be studied separately at a later stage. With this in mind, we first describe the spectral profile of fluorescence for a molecule in the absence of any metal surfaces in terms of a Jablonski diagram, as shown in Figure 1a. An essential feature for the description of the emission (and absorption) spectral profiles is the (vibronic) substructure of the two (ground and excited) singlet states S_0 and S_1; the lowest energy states for each ($S_0(0)$ and $S_1(0)$) being separated by ω_0. We assume the substructure to be approximately continuous and described by a density of states $\rho(\omega_\nu)$ for S_0, where ω_ν is the energy with respect to $S_0(0)$. The molecule is excited by a laser at frequency ω_L, with a photon flux n_L. The number of absorbed photons is $n^0_{abs} = \sigma^0_{abs}(\omega_L)n_L$ (we ignore saturation effects). An electron is excited from $S_0(0)$ to S_1 and then relaxes quickly to $S_1(0)$ (we neglect any thermal population in S_1). It may then relax radiatively to one of the states in S_0, $S_0(\omega_\nu)$, resulting in an emitted photon at a Stokes-shifted frequency $\omega_S = \omega_0 - \omega_\nu$. For a given $\omega_S \le \omega \le \omega_S + d\omega_S$, the transitions $S_1(0) \rightarrow S_0(\omega_\nu = \omega_0 - \omega)$ have a total transition rate $\gamma^0_{Tot}(\omega_S)d\omega_S$. Hence, the overall decay rate of the excited-state is

$$\Gamma^0_{Tot} = \int \gamma^0_{Tot}(\omega_S)d\omega_S \qquad (1)$$

$\gamma^0_{Tot}(\omega_S)d\omega_S$ is in general the sum of radiative, $\gamma^0_{Rad}(\omega_S)d\omega_S$, and nonradiative, $\gamma^0_{NR}(\omega_S)d\omega_S$, contributions, and the radiative decay rate is then

$$\Gamma^0_{Rad} = \int \gamma^0_{Rad}(\omega_S)d\omega_S \qquad (2)$$

Moreover, the spectral density of radiated power (no. of photons per unit time per Stokes frequency) is

$$n^0_{Rad}(\omega_S) = \frac{\gamma^0_{Rad}(\omega_S)}{\Gamma^0_{Tot}}\sigma^0_{abs}(\omega_L)n_L \qquad (3)$$

This is a trivial generalization of a typical one-wavelength fluorescence model, the main addition being the description of the emission spectral profile. This fluorescence spectrum is directly proportional to $\gamma^0_{Rad}(\omega_S)$, whose ω_S-dependence in normal conditions is governed primarily by the density of states $\rho(\omega_0 - \omega_S)$ in the substructure of S_0 and by the matrix elements of the respective transitions; a well-known aspect of fluorescence.[10]

We now generalize this model to molecules in the vicinity of a metallic object. We ignore here any modification of the energy-level structure that may arise from the interaction (chemical or electromagnetic) with the surface or among molecules. At least two EM effects must still be accounted for:[2−4] (i) The excitation field is modified at the molecule position, resulting in a modified absorption by a local field

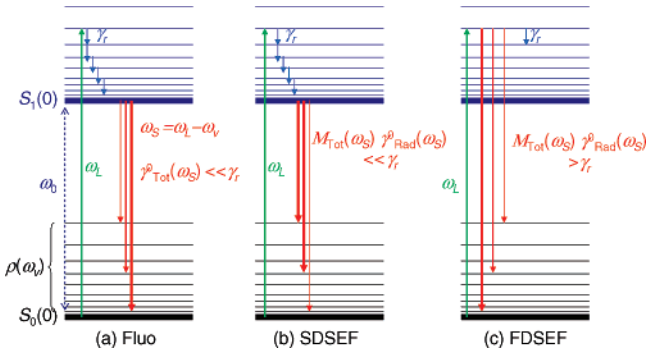

Figure 1. Simplified Jablonski diagrams depicting the processes involved for a fluorophore in three possible situations discussed in the text: (a) standard fluorescence, (b) surface-enhanced fluorescence (SEF) in the slow-dynamics regime (SDSEF), and (c) SEF in the fast-dynamics regime (FDSEF).

enhancement factor $M_{Loc}(\omega_L)$. (ii) The emission properties are strongly altered as follows: the radiative recombination rates $\gamma^0_{Rad}(\omega_S)d\omega_S$ are modified by a factor $M_{Tot}(\omega_S) = M_{Rad}(\omega_S) + M_{NR}(\omega_S)$; part is now emitted into nonradiative modes (i.e., absorbed in the metal) with a rate $M_{NR}(\omega_S)\ \gamma^0_{Rad}(\omega_S)d\omega_S$. The rest constitutes the modified radiative rate: $M_{Rad}(\omega_S)\ \gamma^0_{Rad}(\omega_S)d\omega_S$. To these rates, one should in principle add the intrinsic nonradiative rate $\gamma^0_{NR}(\omega_S)d\omega_S$, which we assume is unaffected by the metal. This is in fact typically negligible compared to $M_{NR}(\omega_S)\ \gamma^0_{Rad}(\omega_S)d\omega_S$ for molecules close to the surface; we will therefore neglect it here. As a result of these rate modifications, the modified overall decay rate of S_1 is

$$\Gamma_{Tot} = \int M_{Tot}(\omega_S)\ \gamma^0_{Rad}(\omega_S)d\omega_S = \bar{M}_{Tot}\Gamma^0_{Rad} \qquad (4)$$

where the second equality, together with eq 2, defines $\bar{M}_{Tot}$. The spectral density of radiated power is now

$$n_{Rad}(\omega_S) = \frac{M_{Rad}(\omega_S)\ \gamma^0_{Rad}(\omega_S)}{\Gamma_{Tot}}M_{Loc}(\omega_L)\ \sigma^0_{abs}(\omega_L)n_L \qquad (5)$$

which may be rewritten in the form of a fluorescence spectral enhancement factor:

$$M_{Fluo}(\omega_S) = \frac{n_{Rad}(\omega_S)}{n^0_{Rad}(\omega_S)} = \frac{M_{Rad}(\omega_S)}{\bar{M}_{Tot}}M_{Loc}(\omega_L) \qquad (6)$$

These considerations are similar to those typically applied to SEF,[3,6,7,11,18] but the ω_S dependence is explicitly included here.[18]

One important (and overlooked) aspect of eq 6 is the ω_S dependence of $M_{Rad}(\omega_S)$. $M_{Rad}(\omega_S)$ exhibits strong resonances (due to LSPs), which are of a width typically comparable to those of fluorescence spectra. In most SEF studies, the emphasis is on matching the LSP resonance to the fluorescence peak, in order to obtain the maximum enhancement.[6,8] Hereafter we focus on situations where this is not the case and highlight two important points: (i) Besides the main fluorescence peak(s), most fluorophores exhibit broad residual emission tails that extend much further toward longer wavelengths; and (ii) $M_{Rad}(\omega_S)$ (and hence $M_{Fluo}(\omega_S)$) can vary over several orders of magnitude (from quenching to enhancement) over a typical emission range. From these two facts, we can envisage an SEF situation where the main fluorescence peak is mostly quenched (or less enhanced), while its tail is enhanced sufficiently to resemble an entirely different fluorescence spectrum, which is then determined mostly by the spectral dependence of $M_{Rad}(\omega_S)$,

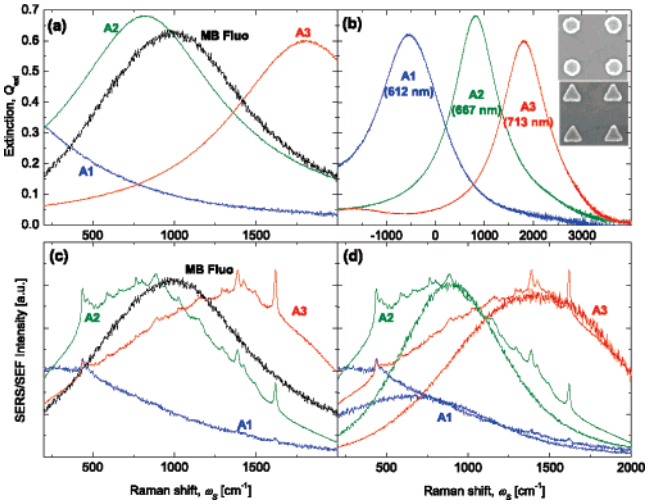

Figure 2. (a and b) Extinction spectra ($Q_{ext}(\omega_S)$) for three gold nanoparticle arrays: A1 (100-nm-edge triangles), A2 (100-nm-diameter dots), and A3 (150-nm-edge triangles). Resonance wavelengths for each are indicated in brackets in b; representative SEM images are shown in the inset. The data in a are the same as in b, but on the same energy scale as used in c and d for easier comparison. (c) SERS/SEF spectra at 633-nm excitation of the same arrays, covered with methylene blue (MB). The standard MB fluorescence (adsorbed on ITO), $P^0_{Fluo}(\omega_S)$, is shown in a and c. (d) Comparison of the SEF spectra of c with the approximated predicted profile: $Q_{ext}(\omega_S)\ P^0_{Fluo}(\omega_S)$.

that is, the LSP resonance profile. Although hints of SPM have been observed in some SEF studies,[6] a case as dramatic as the one described above has not yet been reported to the best of our knowledge.

The main difficulty in providing clear experimental evidence for such a large SPM is to find a substrate where the LSP resonances, and therefore $M_{Rad}(\omega_S)$, are sufficiently well-defined (and uniform across the sample), to extract their influence on the fluorescence spectra. To this end, we have used nanolithographic arrays of gold nanoparticles. The high uniformity can be seen in SEM images (these samples have been described in more detail previously[25]) and confirmed from SERS maps with a high magnification objective ($\times$100). We chose to use single nanoparticles (as opposed to coupled objects) to minimize the unavoidable spatial distribution of enhancement factors over the surface. In order to study particles with different resonances, we investigated various sizes and shapes. Experimental results for methylene blue (MB) adsorbed on three different arrays are shown in Figure 2. The wide backgrounds in Figure 2c are attributed to MB fluorescence (more exactly to SEF with SPM), on the following basis: (i) No SERS/Fluorescence signal is observed in the absence of molecules (after plasma cleaning of the arrays), and (ii) the SEF signal (and SERS peaks) decays as a result of photobleaching of the MB molecules. Moreover, following our model the SEF spectral dependence should be determined by the product $M_{Rad}(\omega_S)P^0_{Fluo}(\omega_S)$,where $P^0_{Fluo}(\omega_S) \propto n^0_{Rad}(\omega_S)$ is the nonmodified fluorescence spectrum. One expects $M_{Rad}(\omega_S)$ to exhibit the same resonances as the extinction spectra $Q_{ext}(\omega_S)$ of the array but not necessarily to be identical to it. An additional probe of $M_{Rad}(\omega_S)$, therefore, comes from the SERS peak intensities. In fact, these peaks exhibit an enhancement factor $M_{Rad}(\omega_S)\ M_{Loc}(\omega_L)$.[24] Using this property, we have shown recently[25] that, for these arrays of noninteracting particles, the extinction spectrum is indeed a good representation of the spectral profile: that is, $M_{Rad}(\omega_S) \propto Q_{ext}(\omega_S)$ to a good approximation. We therefore compare in Figure 2d the SEF/SERS spectra of Figure 2c, with the product $Q_{ext}(\omega_S)\ P^0_{Fluo}(\omega_S)$ (a similar figure for Crystal Violet is provided in Supporting Information Section S.I.). The overall agreement between the predicted and measured spectral profiles further confirms the interpretation of the backgrounds in terms of SEF with a large SPM.

The predictions, however, tend to underestimate slightly the short-wavelength side of the modified SEF spectra (see Figure 2d). This discrepancy could have many possible origins including a slight chemical or EM modification of the energy levels and therefore of the intrinsic fluorescence spectrum of MB upon adsorption, or a small deviation of $M_{Rad}(\omega_S)$ from $Q_{ext}(\omega_S)$. Although we do not exclude these possibilities, we also propose an alternative and novel mechanism, which involves an even more drastic modification of the fluorescence of molecules close to metallic surfaces, and which we call fast-dynamics SEF (FDSEF); the previous situation being then referred to as slow-dynamics SEF (SDSEF). The rationale for introducing this new type of SEF is as follows: previously we have made the common assumption that following excitation to S_1 the excited electron relaxes quickly to $S_1(0)$, from where the different decay paths follow. This is entirely justified in normal conditions, where the overall lifetime of S_1 is typically $\sim$0.1$-$10 ns, that is, much longer than internal relaxation times in S_1 ($\sim$1 ps). There may be situations close to metals, however, where the total decay rate of S_1 is enhanced sufficiently to become comparable to the internal relaxation rates.[1,7,26] (See Supporting Information Section S.II. for a detailed discussion.) In this case, the excited electron does not have time to relax down to $S_1(0)$ and radiative decays may occur from higher levels $S_1(\omega_v)$ in the substructure of S_1.

A quantitative model of FDSEF is more difficult because at each step in the relaxation process there is a competition between decay to S_0 and internal relaxation carried over to the next step down in the energy ladder (see Figure 1c). We therefore only discuss the effect qualitatively. Let us consider the limiting case where all decay rates from $S_1(\omega_v)$ are much faster than internal relaxation (ultrafast dynamics SEF, UFDSEF). All decays will then occur from state $S_1(\omega_L - \omega_0)$,instead of $S_1(0)$, see Figure 1c. This reduces in a first approximation to the same problem as before for SDSEF (Figure 1b), except that the nonmodified fluorescence spectrum, $n^0_{Rad}(\omega_S)$, must be considered as blue-shifted by an energy $\omega_L - \omega_0$. This blue-shifted fluorescence spectrum remains affected by the factor $M_{Rad}(\omega_S)$, and its spectral shape may therefore be modified, that is

$$n_{Rad}(\omega_S) \approx \frac{M_{Rad}(\omega_S)\ n^0_{Rad}(\omega_S - \omega_L + \omega_0)}{\tilde{M}_{Tot}} M_{Loc}(\omega_L) \quad (7)$$

Note that $n^0_{Rad}(\omega_S - \omega_L + \omega_0)$ is the intrinsic fluorescence profile, but peaking at ω_L instead of ω_0. It will therefore be basically the same for many typical fluorophores, whose fluorescence spectral profile are similar except for the actual peak position. Accordingly, the UFDSEF spectral profile is in this case (to a large extent) independent of the intrinsic fluorescence of the molecule under investigation. Finally, for intermediate cases where the modified decay rates of S_1 are comparable to the internal relaxation rates, one can expect qualitatively an intermediate situation between SDSEF and the extreme case of UFDSEF discussed above. In all cases, an FDSEF spectrum should resemble the corresponding SDSEF emission, but either blue-shifted or with a tail biased toward higher energies.

A clear-cut experimental demonstration of FDSEF (or UFDSEF) without invoking time-resolved studies is difficult

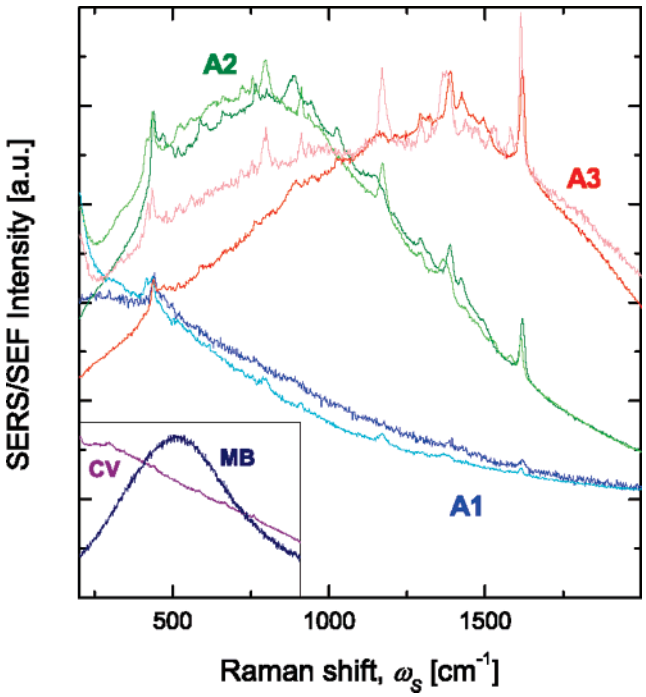

Figure 3. Comparison of the SERS/SEF spectra of MB and CV (light-colored lines, recognizable by the two prominent SERS peaks at 800 and 1170 cm^{-1}) on arrays A1, A2, and A3. The intrinsic fluorescence spectra (at 633 nm) are shown in the inset.

for several reasons. The spatial distribution of the enhancement factors results in only part of the molecules being under FDSEF conditions (the rest showing SDSEF), and distinguishing between the two contributions would require single-molecule experiments. Still, such a mixed SDSEF/FDSEF signal could account qualitatively for the small deviations between the predicted SDSEF spectra and the measurements in Figure 2d, which are consistent with FDSEF for at least part of the molecules. Again, distinguishing clearly the SDSEF and FDSEF spectra is difficult because of their strong similarity. Both result in a spectral profile that is dominated primarily by $M_{\mathrm{Rad}}(\omega_S)$, the influence of the intrinsic fluorescence $P^0_{\mathrm{fluo}}(\omega_S)$ being more important for SDSEF, but remaining in most cases secondary. Despite this, we do observe a hint of this difference when comparing the SEF/SERS spectra of two dyes, Crystal Violet (CV) and MB, each with a very different intrinsic fluorescence at 633 nm (see the inset of Figure 3). FDSEF should be more dominant for arrays where the enhancement factors are large at ω_L, that is for A1 and A2 compared to A3 (see Supporting Information Section S.II.). The SEF spectra of CV and MB on A1 and A2 are indeed very similar, see Figure 3, as expected for FDSEF spectra. This is not so much the case for A3, which suggests that SDSEF (which is more influenced by the intrinsic fluorescence) has a larger contribution.

Finally, we conclude by proposing that SEF (either SDSEF with a large SPM or FDSEF) may be the origin of the so-called SERS continuum in many common situations. Previous studies[17,19−21] have in fact already shown that SEF could account for part of the SERS continuum, but not for all of it. We believe that these additional contributions can still be attributed to SEF if one allows the possibility of a large SPM and/or of FDSEF; an interpretation that could in fact reconcile apparently discordant observations.[17,21−23] Additional arguments in favor of this interpretation are given in Supporting Information Section S.III. Further investigations are required to confirm this view.

Acknowledgment. This work was supported by the Dumont d'Urville France/NZ exchange programme. We are indebted to A. Hohenau and J. Krenn from Karl Franzens University (Graz, Austria) where the samples were fabricated.

Supporting Information Available: Section S.I provides a figure equivalent to Figure 2d but for crystal violet (CV) instead of methylene blue (MB), along with a brief discussion. Section S.II provides estimations of the modified decay rates in typical situations. It is shown that situations of FDSEF should be common and that the FDSEF/SDSEF signals should be comparable to their SERS counterparts; thus justifying our proposal that it must contribute to a substantial fraction (if not all) of the observed SERS backgrounds, a proposal that is discussed further in Section S.III. This material is available free of charge via the Internet at http://pubs.acs.org.

References and Notes

(1) Philpott, M. R. *J. Chem. Phys.* **1975**, *62*, 1812.
(2) Chance, R. R.; Prock, A.; Silbey, R. *Adv. Chem. Phys.* **1978**, *37*, 1.
(3) Metiu, H. *Progress. Surf. Sci.* **1984**, *17*, 153; and references therein.
(4) Ford, G. W.; Weber, W. H. *Phys. Rep.* **1984**, *113*, 195; and references therein.
(5) Dulkeith, E.; Morteani, A. C.; Niedereichholz, T.; Klar, T. A.; Feldmann, J.; Levi, S. A.; van Veggel, F. C. J. M.; Reinhoudt, D. N.; Möller, M.; Gittins, D. I. *Phys. Rev. Lett.* **2002**, *89*, 203002.
(6) Kühn, S.; Hakanson, U.; Rogobete, L.; Sandoghdar, V. *Phys. Rev. Lett.* **2006**, *97*, 017402.
(7) Anger, P.; Bharadwaj, P.; Novotny, L. *Phys. Rev. Lett.* **2006**, *96*, 113002.
(8) Tam, F.; Goodrich, G. P.; Johnson, B. R.; Halas, N. J. *Nano Lett.* **2007**, *7*, 496.
(9) Novotny, L.; Hecht, B. *Principles of Nano-Optics*; Cambridge University Press: Cambridge, 2006.
(10) Lakowicz, J. R. *Principles of Fluorescence Spectroscopy*, 3rd ed.; Springer: New York, 2006.
(11) Das, P.; Metiu, H. *J. Phys. Chem.* **1985**, *89*, 4680.
(12) Zhao, J.; Jensen, L.; Sung, J.; Zou, S.; Schatz, G. C.; Van Duyne, R. P. *J. Am. Chem. Soc.* **2007**, *129*, 7647.
(13) Lombardi, J. R.; Birke, R. L.; Lu, T.; Xu, J. *J. Chem. Phys.* **1986**, *84*, 4174.
(14) Fuchs, R.; Barrera, R. G. *Phys. Rev. B* **1981**, *24*, 2940.
(15) Bellessa, J.; Bonnand, C.; Plenet, J. C.; Mugnier, J. *Phys. Rev. Lett.* **2004**, *93*, 036404.
(16) Knoll, W.; Philpott, M. R.; Swalen, J. D.; Girlando, A. *J. Chem. Phys.* **1982**, *77*, 2254.
(17) Maruyama, Y.; Futamata, M. *J. Raman Spectrosc.* **2005**, *36*, 581.
(18) Enderlein, J. *Phys. Chem. Chem. Phys.* **2002**, *4*, 2780.
(19) Xu, H. et. al. *Phys. Rev. Lett.* **2004**, *93*, 243002.
(20) Johansson, P.; Xu, H.; Käll, M. *Phys. Rev. B* **2005**, *72*, 035427.
(21) (a) Itoh, T. et al. *J. Chem. Phys.* **2006**, *124*, 134708. (b) Itoh, T. et. al *J. Phys. Chem. B* **2006**, *110*, 21536. (c) Itoh, T. et. al *J. Photochem. Photobiol., A* **2006**, *183*, 322.
(22) Moskovits, M. *J. Raman Spectrosc.* **2005**, *36*, 485.
(23) Jiang, J.; Bosnick, K.; Maillard, M.; Brus, L. *J. Phys. Chem. B* **2003**, *107*, 9964.
(24) Le Ru, E. C.; Etchegoin, P. G. *Chem. Phys. Lett.* **2006**, *423*, 63.
(25) Le Ru, E. C.; Etchegoin, P. G.; Grand, J.; Félidj, N.; Aubard, J.; Lévi, G.; Hohenau, A.; Krenn, J. R. *Curr. Appl. Phys.*, in press.
(26) Leitner, A.; Lippitsch, M. E.; Aussenegg, F. R. In *Surface Studies with Lasers*; Springer: New York, 1983.

Supporting information for "The mechanisms of spectral profile modification in Surface Enhanced Fluorescence"

S.I. ADDITIONAL EXPERIMENTAL RESULTS FOR CRYSTAL VIOLET

The discussion of Slow-Dynamics SEF (SDSEF) in the main text focuses on the case of methylene blue (MB) because its non-modified fluorescence spectrum is centered in the region of interest and any modification (shift) may be viewed as more "spectacular". We discuss briefly in this supporting information the case of crystal violet (CV), whose non-modified fluorescence is centered below the laser energy, i.e. our monitored wavelength range lies in the tail of the non-modified fluorescence spectrum.

Fig. S1 is the equivalent of Fig. 2(d) of the main text, but for CV instead of MB. A large Spectral Profile Modification (SPM) of the fluorescence is clearly observed, and as for MB, it follows the underlying Localized Surface Plasmon (LSP) resonance, and can be predicted, at least semi-quantitatively, by the simple model described in the main text. The case of CV, however, is quite particular and therefore not ideal for further interpretation. Firstly, in the case where only the fluorescence tail is monitored (as for CV), the SDSEF and Fast-Dynamics SEF (FDSEF) signals should be very similar, since the blue-shift of the tail-like non-modified fluorescence results in a tail-like spectral profile. The SDSEF model proposed in the text should therefore also apply approximately to FDSEF for CV. This may be the reason why the agreement between experiment and prediction is better than for MB for arrays A1 and A2, as seen in Fig. S1. Secondly, CV is also known to exhibit an extremely fast non-radiative relaxation ($\sim 1\,$ps) from the first excited state to the ground state (comparable to internal relaxation in the excited state). This should have no effect on FDSEF (or at least UFDSEF), where the modified decay rates dominates entirely the dynamics. But it may affect the dynamics in "normal" fluorescence conditions, and our simple SDSEF model may therefore not apply to CV. This may explain the discrepancy between prediction and experiment for array A3, where SDSEF is expected to be more prominent over FDSEF (see Sec. S.II).

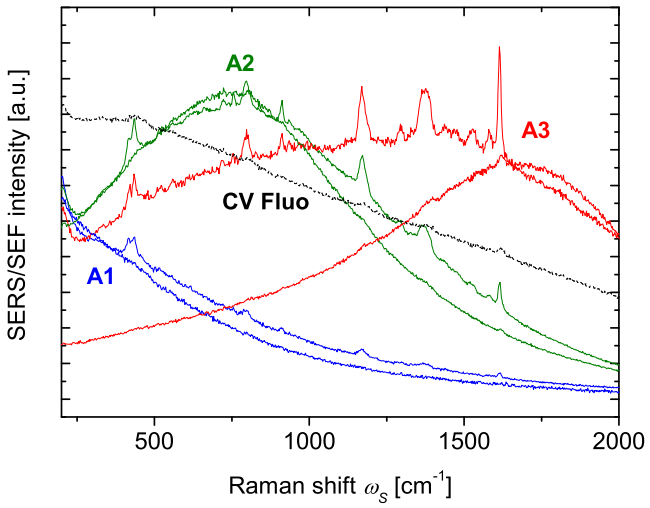

FIG. S1: This figure is the equivalent of Fig. 2(d) of the main text, but for crystal violet (CV). It shows the comparison between the SERS/SEF and the approximated predicted profile within the SDSEF framework: $Q_{\rm ext}(\omega_S)P^0_{\rm Fluo}(\omega_S)$. Also shown here (black dotted line) is the (non-modified) fluorescence spectrum of pure CV (adsorbed on ITO).

S.II. ESTIMATIONS OF DECAY RATE MODIFICATION IN S1

The modified decay rate in the excited state for slow-dynamics SEF (SDSEF) is given in Eq. (4) of the main text. It is characterized by the decay rate enhancement factor $\bar{M}_{\rm Tot}$, which itself depends on the frequency-dependent decay rate enhancement factor $M_{\rm Tot}(\omega_S)$. One can see from Eq. (4) that if $M_{\rm Tot}(\omega_S)$ do not vary much across the fluorescence spectrum, then $\bar{M}_{\rm Tot} \approx M_{\rm Tot}(\omega_S)$. One can therefore estimate in a first approximation $\bar{M}_{\rm Tot}$ for any molecule by approximating it with $M_{\rm Tot}(\omega_F)$, where $\omega_F \approx \omega_0$ is the center frequency of the fluorescence spectrum. The modified decay rate is then given by

$$\Gamma_{\rm Tot} \approx M_{\rm Tot}(\omega_F)\Gamma^0_{\rm Rad}, \qquad \text{(S1)}$$

where $\Gamma^0_{\rm Rad}$ is the non-modified radiative decay rate. For typical fluorophores, $(\Gamma^0_{\rm Rad})^{-1}$ is of the order of $1-10\,$ns. For example, for rhodamine 6G,[1] $\Gamma^0_{\rm Rad} = \Gamma^0_{\rm Tot} \approx (4{\rm ns})^{-1}$ since its quantum yield is close to 1. For methylene blue,[2] $\Gamma^0_{\rm Tot} = (345{\rm ps})^{-1}$, which given its quantum yield of ≈ 0.02 gives $\Gamma^0_{\rm Rad} = (17{\rm ns})^{-1}$.

In the case of Fast-Dynamics SEF (FDSEF), the modified decay rate may vary slightly depending on how far down the electron has already relaxed (between $S_1(\omega_L-\omega_0)$ and $S_1(0)$). In the limiting case of Ultra-Fast-Dynamics SEF (UFDSEF), all emission occurs from $S_1(\omega_L-\omega_0)$ and the relevant decay rate EF should therefore be estimated, not at ω_F as for SDSEF, but at frequency $\omega_F+\omega_L-\omega_0 \approx \omega_L$, i.e. at the laser frequency.

Moreover, typical internal relaxation times (comparable to vibrational lifetimes) in fluorophores are of the order $1-10\,$ps. We therefore conclude that, in general, total decay rate EFs of the order of $M_{\rm Tot} \approx 10^3$ are necessary to observe any FDSEF. Moreover, for EFs as large as 10^4-10^5, then UFDSEF can be expected.

We will in the following calculate $M_{\rm Tot}(\omega)$ for a few model examples. The aim is twofold: firstly to show

that the conditions required for FDSEF to exist are, at least theoretically, common, in particular for molecules adsorbed on a metallic surface. Secondly, and this point is related to the previous one, we will argue that SEF is possible even for molecules directly adsorbed on the metal (which is necessary if any FDSEF signal is to be observed). This is usually assumed not to be the case because of the large non-radiative quenching, but we will show that it is not necessarily so.

We start by recalling briefly the basic EM effects for a fluorophore close to a metallic surface and how they relate to SERS and SEF. Several approximations are made in these expressions and they should therefore be viewed as only semi-quantitative, for order of magnitude estimates only. More details can be found for example in Refs. 3,4.

A. The various enhancement factors

When a molecule is in the vicinity of a metal surface, various processes are modified and such changes are characterized by an enhancement factor (EF) (note that the EFs also characterize any quenching rather enhancement):

- The local field E_{Loc} (felt at the molecule position) is modified compared to the incident local field E_0 by a local field enhancement factor:

$$M_{\mathrm{Loc}} \approx \frac{|E_{\mathrm{Loc}}|^2}{|E_0|^2} \tag{S2}$$

  This EF characterizes in particular the modification of the absorption cross-section.

- The total decay rate of the emitter at a given frequency is modified by a total decay rate EF M_{Tot}. M_{Tot} can be decomposed as the sum of two EFs corresponding to radiative and non-radiative emission: $M_{\mathrm{Tot}} = M_{\mathrm{Rad}} + M_{\mathrm{NR}}$. The quantum yield for emission is then modified. If the non-radiative channel characterized by M_{NR} is dominant over any intrinsic non-radiative decay of the molecule, then the modified quantum yield is simply $Q = M_{\mathrm{Rad}}/M_{\mathrm{Tot}}$.

We also note that M_{Loc} and M_{Rad} can be linked using the Optical Reciprocity Theorem.[3,4] Without going into too much details, one can in a first approximation consider that M_{Loc} and M_{Rad} (at a given position and frequency) are of the same order of magnitude.

In SEF, the signal is enhanced firstly by the local field EF (which enhances the absorption rate). Because the emission process in SEF is a competition between the radiative and non-radiative channels, the emission is characterized by the modified quantum yield, Q. The overall fluorescence enhancement factor is therefore:[3]

$$M_{\mathrm{Fluo}} \approx M_{\mathrm{Loc}} Q \approx M_{\mathrm{Loc}} \frac{M_{\mathrm{Rad}}}{M_{\mathrm{Tot}}} \tag{S3}$$

Because SERS is a scattering process, the non-radiative SERS emission does not compete with the radiative emission, the SERS EF is therefore[3–5]:

$$M_{\mathrm{SERS}} \approx M_{\mathrm{Loc}} M_{\mathrm{Rad}} \tag{S4}$$

B. Examples of predicted decay rate enhancement factor

M_{Tot} and M_{Rad} can be calculated within classical EM theory. Exact results are obtainable in special cases and we here focus on three examples for dipole emission close to:

- a planar metal surface,[6,7]
- a metallic sphere[8] using Mie theory,
- or a pair of metallic spheres (dimer), using Generalized Mie Theory[9,10].

Fig. S2(a-c) shows the results of such predictions for a few representative cases, see caption for details. The metal is gold and its dielectric function is taken as given in Ref. 11. Only the case of a dipole perpendicular to the surface, at a distance d from the surface, is shown for clarity since the conclusions for a parallel dipole are similar. For an emitter very close to the metal surface (typically less than 5 nm), we conclude from these model examples (and from a more detailed study of the influence of the various parameters, not shown here) the following:

- For the plane and the sphere, $M_{\mathrm{Tot}} \gg M_{\mathrm{Rad}}$, i.e. $M_{\mathrm{Tot}} \approx M_{\mathrm{NR}}$, and $Q \ll 1$. M_{Tot} is then mostly determined by the distance between the metal surface and the emitter, independently of the actual geometry –and therefore of the Localized Surface Plasmon (LSP) resonances– of the metallic object. Its frequency dependence is therefore essentially governed by the intrinsic optical properties of the metal, while its magnitude depends on the distance as d^{-3}.

- M_{Tot} can be quite large, $\approx 10^5$ for $d = 1$ nm at the non-radiative resonance around 500 nm for gold in air (corresponding to $\epsilon = -1$). Around 650 nm (the region of interest to us), M_{Tot} is still of the order of $10^3 - 10^4$. M_{Tot} would be even larger for a dipole closer to the surface, although a non-local dielectric function should then be used for quantitative predictions.

- For the gold dimer, M_{Rad} becomes comparable to the M_{Tot} predicted for the plane, and M_{Rad} then contributes significantly to M_{Tot}. In particular, resonances of M_{Rad} are then observed in M_{Tot}, and M_{Tot} has a relatively large radiative component, i.e. $Q > 0.1$. Moreover, in this case of very large field enhancement, M_{Tot} can be even larger than in the typical cases of the plane and sphere discussed above.

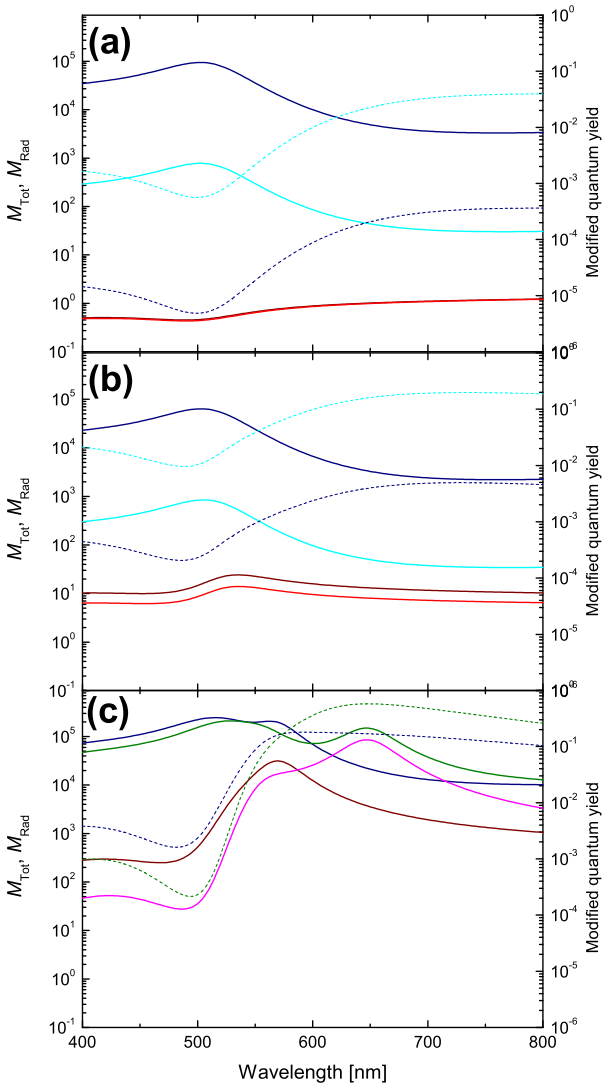

FIG. S2: Predictions of the frequency dependence of $M_{\rm Tot}$ (blue), $M_{\rm Rad}$ (red) (solid lines, both scale on the left axis), and the modified quantum yield (dotted lines, scale on the right axis) for a dipole in air perpendicular to a gold metal surface and at a distance d from the surface. Three examples are given (a) A semi-infinite gold plane in air. (b) A gold nano-sphere of radius $a = 30\,$nm in air. (c) A dimer of two gold nano-spheres of radius $a = 30\,$nm, and separated by a gap of $2\,$nm. The dipole is placed in the middle of the gap in this latter case ($d = 1$). The dimer in air case is shown in dark blue and dark red, while the dimer in water is also shown in green ($M_{\rm Tot}$ and Q) and pink ($M_{\rm Rad}$). Two distances are shown in (a) and (b): $d = 1\,$nm (dark blue and dark red), and $d = 5\,$nm (light blue and light red). Vertical scales have been kept the same for all three plots.

We conclude that, in typical situations, $M_{\rm Tot}$ can easily be large enough for FDSEF to exist, and even possibly UFDSEF. This is particularly true for the first few monolayers, i.e. at distances of the order of $d \approx 1\,$nm or less from the surface.

C. Predicted intensity of the FDSEF signal

We must however now consider whether in such situations, any detectable fluorescence is expected. It is indeed often assumed that at such short distances the fluorescence signal would be completely quenched because of the dominance of non-radiative decay. This dominance is indeed a fact in many situations and results in very poor modified quantum yields, Q, as evidenced in Fig. S2(a-b), but it does not necessarily imply a complete quenching of the SEF signal.

To understand this, we focus on the approximate expressions for the EF of fluorescence and SERS, given in Eqs. S3 and S4 and recall that $M_{\rm Loc}$ is of the same order as $M_{\rm Rad}$. We consider an emitter (SERS and SEF) very close to the surface, say $d = 1\,$nm for the sake of argument.

Let us first consider the case of a planar surface (see Fig. S2(a)). $M_{\rm Rad}$ and $M_{\rm Loc}$ are of the order of 1, while $Q < 10^{-3}$, so that $M_{\rm Fluo} \approx 10^{-3} - 10^{-4}$. It is clear in this case that a large fluorescence quenching occurs, and this is partly the origin of the common view that fluorescence near metal surfaces is always quenched. Even if FDSEF exists in such a case, its intensity would not be detectable. Note in passing that no SERS enhancement is expected either, but no quenching of the Raman signal should occur, $M_{\rm SERS} \approx 1$.

The situation is similar in the case of a gold sphere, because the radiative (and local field) enhancements remain small compared to $M_{\rm Tot}$ for $d = 1\,$nm. It is interesting to note at this stage that this is not true for a silver sphere, for which the LSP resonances are much stronger (and the local field and radiative enhancements accordingly much larger), see Ref. 3 for more detail. This highlights one important aspect of the optical properties of gold. Because of the large absorption for $\lambda < 600\,$nm, the LSP resonances are strongly damped. At longer wavelength however, the optical absorption of gold becomes comparable with that of silver, and much stronger LSP resonances (and therefore EFs) are then possible. To profit from these, one must have a gold structure where the LSP resonances are red-shifted to this region. This can for example be achieved by using non-spherical structures (like the ones used in the main paper), by placing the structures on dielectric substrate (such as ITO as in the structures of the main paper), by making interacting structures, or by embedding the structures in a dielectric of larger dielectric constant (like water).

For easier calculations, we have presented results in Fig. S2(c) where the resonances have been red-shifted by using interacting objects (a dimer) and placing it in water. This results in much stronger resonances and much larger EFs. The same conclusions would be obtained for any structures where the resonances have been shifted toward the lower absorption region $\lambda > 600\,$nm, providing there are positions of sufficiently large local field EFs. The existence of a large local field EF on the surface structure can be inferred qualitatively by the observa-

tion of a SERS signal (as in the structures presented in the main text). As illustrated in Fig. S2(c), it is then possible to have M_{Rad} almost comparable to M_{Tot}, and therefore a modified quantum yield of the order of $\sim 0.1-1$, even for an emitter as close as 1 nm to the surface. No quenching of the fluorescence signal is therefore predicted, and even enhancements are possible (depending on how close the dipole is to the surface). It should therefore be possible to observe the fluorescence signal, even in FDSEF or UFDSEF conditions.

Finally, the SERS EF is predicted to be of the order of M_{Tot} larger than M_{Fluo}, say larger by a factor of $\sim 10^5 - 10^6$. But for a typical fluorophore, the non-modified fluorescence cross-section is $\sim 10^{10}$ larger than the non-modified Raman cross-section.[5] The (integrated) SEF signal should therefore be $\sim 10^4$ times larger than the SERS signal, but it is also spread out over a much larger ($\sim 10^2 - 10^3$) spectral range than a typical SERS peak. These considerations, although mostly qualitative, show that it is not surprising that for molecules adsorbed on the metal, the SEF signal (which could be misinterpreted as a SERS background) is of the order of the SERS peaks, the relative intensity depending on the actual distance of the emitter from the surface.

D. A note on the FDSEF vs SDSEF contribution

In most metallic substrates, there is a wide distribution of EFs on the surface.[12,13] Hence, it is likely (except may be in single molecule conditions) that any FDSEF signal be accompanied by some SDSEF signal (from those molecule subjected to smaller enhancement factors). The relative contribution of FDSEF vs. SDSEF will vary with the exact experimental conditions and in particular with the LSP resonance properties of the substrate. In simple terms, the stronger the resonances (and the associated EFs), the more FDSEF should be observed. However, as mentioned earlier in this section, what is important for FDSEF is M_{Tot} at the laser frequency ω_L (this applies strictly speaking to UFDSEF, FDSEF being an intermediate case between UFDSEF and SDSEF). One could therefore expect qualitatively that those substrates with a resonance closer to the laser frequency (A1 and A2 in our study) are more dominated by FDSEF rather than SDSEF. This is the effect that is tentatively shown in Fig. 3 of the main text. Moreover Further experiments are necessary to place these qualitative arguments on a firmer footing.

S.III. INTERPRETING THE SERS CONTINUUM IN TERMS OF SDSEF/FDSEF

As mentioned in the main text, we believe that SEF (either SDSEF with a large SPM or FDSEF) may be the origin of the so-called SERS continuum in many common situations. Such an interpretation is compatible with many well-known features of the SERS continuum,[14–17] which we list below along with other important predictions of this proposal:

- The SDSEF/FDSEF follows the same intensity fluctuations and polarization properties of the SERS signal through the factor $M_{\mathrm{Rad}}(\omega_S)$, as observed for the SERS continuum.

- There is no SEF in the absence of adsorbed molecules, as for the SERS continuum. We note that this is still a contentious point in relation to the SERS continuum itself, since there are conflicting reports of whether the SERS continuum is observed or not in the absence of adsorbed molecules. These have been tentatively attributed to problems of surface cleanness and impurities.[18] Our experiments support this view: the SEF/SERS background only disappears upon thorough plasma cleaning.

- The issue of surface cleanness and impurities is even more problematic for non-resonant molecules, since the SERS signals are much smaller[5] and therefore potentially more affected by contaminations. The SEF from organic impurities[18] could therefore account for the SERS background of non-resonant molecules.

- Contrary to what is generally thought, SEF is possible even for molecules in direct contact with the metal, as often the case in SERS. This was shown and discussed in Sec. S.II.

- The underlying resonance that should characterize the SPM of the SEF (and therefore the SERS background within our proposal) is not seen in most SERS experiments because of its large inhomogeneous broadening for most substrates and the typically small spectral window usually probed with high dispersion gratings. Our ability to identify it as such in Fig. 2(c) of the main text is a direct consequence of the high uniformity of the resonances in our structures and the wide spectral window.

- As mentioned in the main text, in UFDSEF conditions, the spectral profile is mostly independent of the molecule, and could therefore account for the lower energy peak of the SERS continuum observed in Ref. 14 (previously attributed to electronic Raman scattering or to LSP luminescence).

- One interesting consequence of the SEF interpretation concerns the behavior of the SERS background when changing laser excitation. Depending on the specific SERS conditions, the background may consist of either SDSEF, FDSEF, or both. When changing excitation wavelength, the SDSEF signals should retain their spectral profile, but the FDSEF should be shifted together with the laser

in a similar fashion as a Raman signal, thus potentially explaining conflicting reports regarding the actual nature (Raman vs. luminescence) of the SERS background.

[1] Eggeling, C.;Widengren, J.;Rigler, R.;M. Seidel, C. A. *Anal. Chem.* **1998**, *70*, 2651.
[2] Atherton, S. J.;Harriman, A. *J. Am. Chem. Soc.* **1993**, *115*, 1816.
[3] Le Ru, E. C.; Etchegoin, P. G. **2005**, arXiv:physics/0509154v1.
[4] Le Ru, E. C.; Etchegoin, P. G. *Chem. Phys. Lett.* **2006**, *423*, 63.
[5] Le Ru, E. C.; Blackie, E.; Meyer, M.; Etchegoin, P. G. *J. Phys. Chem. C* **2007**, *in press*, DOI:10.1021/jp0687908.
[6] Chance, R. R.; Prock, A. ; Silbey, R. *Adv. Chem. Phys.* **1978**, *37*, 1.
[7] Novotny, L.; Hecht, B. *Principles of Nano-Optics* (Cambridge University Press, Cambridge, 2006).
[8] Chew, H. *J. Chem. Phys.* **1987**, *87*, 1355.
[9] Gérardy, J. M.; Ausloos, M. *Phys. Rev. B* **1982**, *25*, 4204.
[10] Johansson, P. ; Xu, H. ; Käll, M. *Phys. Rev. B* **2005**, *72*, 035427.
[11] Etchegoin, P. G.; Le Ru, E. C.; Meyer, M. *J. Chem. Phys.*, **2006**, *125*, 164705.
[12] Le Ru, E. C.; Etchegoin, P. G.; Meyer, M. *J. Chem. Phys.*, **2006**, *125*, 204701.
[13] Le Ru, E. C.; Meyer, M.; Etchegoin, P. G. *J. Phys. Chem. B*, **2006**, *110*, 1944.
[14] Y. Maruyama and M. Futamata, J. Raman Spectrosc. **36**, 581 (2005).
[15] Itoh, T. *et al. J. Chem. Phys.* **2006**, *124*, 134708; Itoh, T. *et. al J. Phys. Chem. B* **2006**, *110*, 21536; Itoh, T. *et. al*, *J. Photochem. Photobio. A* **2006**, *183*, 322.
[16] Moskovits, M. *J. Raman Spectrosc.* **2005**, *36*, 485.
[17] Jiang, J.; Bosnick, K.; Maillard, M.; Brus, L. *J. Phys. Chem. B* **2003**, *107*, 9964.
[18] Y. Maruyama and M. Futamata, Chem. Phys. Lett. **2005**, *412*, 65.